Identification of the Catalytic Residues Involved in the Carboxyl Transfer of Pyruvate Carboxylase

Jin Yong-Biao, Md. Nurul Islam, Shinji Sueda,* and Hiroki Kondo

Department of Biochemical Engineering and Science, Kyushu Institute of Technology, Iizuka 820-8502, Japan

Received October 2, 2003; Revised Manuscript Received March 23, 2004

ABSTRACT: To clarify the mechanism of carboxyl transfer from carboxylbiotin to pyruvate, the following conserved amino acid residues present in the carboxyl transferase domain of *Bacillus thermodenitrificans* pyruvate carboxylase were converted to homologous amino acids: Asp543, Glu576, Glu592, Asp649, Lys712, Asp713, and Asp762. The carboxylase activity of the resulting mutants, D543E, E576D, E576Q, E592Q, D649N, K712R, K712Q, D713E, D713N, D762E, and D762N, was generally less than that of the wild type from mutation, but it decreased the most to 5% or even less than that of the wild type with D543E, D576Q, D649N, K712R, and K712Q. The decrease in activity observed for Asp543, Asp649, and Lys712 mutants was not for structural reasons because their structures seemed to remain intact as assessed by gel filtration and circular dichroism. On the basis of these data, a mechanism is proposed where Lys712 and Asp543 serve as the key acid and base catalyst, respectively.

Pyruvate carboxylase (PC, EC 6.4.1.1)[1] is a biotin-dependent enzyme and is involved in gluconeogenesis by converting pyruvate to oxalacetate (*1*). PC is distributed widely in both eukaryotes and some prokaryotes but in two different forms (*2*, *3*). One form of PC, found in eukaryotes and some prokaryotes, is made of a single polypeptide chain of about 1200 amino acids. The other form of PC, found only in prokaryotes, consists of two polypeptide chains with the total amino acid residues similar to that of the former (*3*). The reaction of PC is believed to proceed in two steps, just like those of other biotin-dependent carboxylases such as acetyl-CoA carboxylase (ACC): carboxylation of enzyme-bound biotin by bicarbonate and ATP and subsequent transfer of the carboxyl group to pyruvate from carboxylated biotin (*4*).

$$\mathrm{ATP} + \mathrm{HCO_3^-} + \mathrm{Enz{-}biotin} \rightleftharpoons \mathrm{Enz{-}biotin{-}CO_2^-} + \mathrm{ADP} + \mathrm{Pi} \quad (1)$$

$$\mathrm{Enz{-}biotin{-}CO_2^-} + \mathrm{pyruvate} \rightleftharpoons \mathrm{Enz{-}biotin} + \mathrm{oxalacetate} \quad (2)$$

Thus, PC carries at least three functional domains: a biotin-carrying unit, biotin carboxylase (BC) domain, which mediates the first partial reaction (eq 1), and carboxyl transferase (CT) domain, which catalyzes the second partial reaction (eq 2). The BC domain of the single polypeptide chain PC is located in the amino terminus, followed by the CT domain with the biotin-carrying domain residing in the carboxyl terminus (*5*). In the subunit-type PC, the polypeptide chain is divided between the BC and CT domains (*6*). In addition, the activity of the former class of PC is modulated by acetyl-CoA and aspartate, but the latter class of PC is insensitive to these agents. Because of the lack of three-dimensional structural information, the detailed mechanism of carboxylation by PC and its allosteric regulation are not known. Obviously, elucidation of the three-dimensional structure of PC will unveil much of this ambiguity, and in fact such an undertaking is under way in this laboratory. Along with it, protein engineering approaches may be useful to evaluate the function of individual domains of PC and to unravel the mechanism of reaction and regulation. Herein, some of the conserved residues of the CT domain of *Bacillus thermodenitrificans* (previously referred to as *B. stearothermophilus*) PC were mutated to assess their involvement in catalysis (*7*). A large number of sequence data are now available on biotin-dependent carboxylases: 41 for PC, 24 for prokaryotic ACC, 11 for eukaryotic ACC, 22 for propionyl-CoA carboxylase, and 6 for methylcrotonyl-CoA carboxylase, but conserved residues are scarce, and it is difficult to find sequence homology for their CT domains. Nonetheless, if we assume that, despite poor sequence homology, all of these enzymes mediate carboxyl transfer by an identical or similar mechanism, catalytic residues may be common to all of these enzymes. On the basis of this assumption we end up with only four aspartates (Asp543, Asp649, Asp713, and Asp762), two glutamates (Glu576 and Glu592), and one lysine (Lys712). These residues are readily amenable to site-directed mutagenesis to evaluate their function, and the results are reported below.

EXPERIMENTAL PROCEDURES

Materials. Inorganic salts and common organic chemicals were obtained from commercial sources. Avidin was from

* To whom correspondence should be addressed. Phone: +81-948-29-7834. Fax: +81-948-29-7801. E-mail: sueda@bse.kyutech.ac.jp.

[1] Abbreviation: ACC, acetyl-CoA carboxylase; BC, biotin carboxylase; BCCP, biotin carboxyl carrier protein; Bis-Tris, [bis(2-hydroxyethyl)amino]tris(hydroxymethyl)methane; CD, circular dichroism; CT, carboxyl transferase; DTT, dithiothreitol; IPTG, isopropyl β-thiogalactoside; KPi, potassium phosphate; LB, Luria-Bertani; ORF, open reading frame; PC, pyruvate carboxylase; PCR, polymerase chain reaction; PEP, phosphoenolpyruvate; Tricine, *N*-[tris(hydroxymethyl)-methyl]glycine.

10.1021/bi035783q CCC: $27.50
Published on Web 04/24/2004

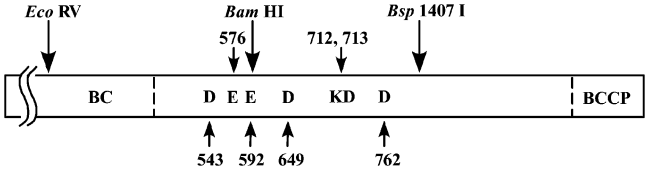

FIGURE 1: Targets of mutagenesis of the CT domain of *B. thermodenitrificans* PC, with the major restriction enzyme sites used for gene manipulation being illustrated.

ProZyme, CA, and acetyl-coenzyme A was from Wako Pure Chemical, Osaka, Japan. Reagents for genetic engineering such as restriction enzymes were purchased from Takara, Kyoto, Japan, and oligonucleotides were custom-synthesized by Hokkaido Science, Sapporo, Japan. The TOPO TA cloning kit was the product of Invitrogen, CA.

Gene Manipulations. B. thermodenitrificans PC gene in pTrc99A vector was used for the mutagenesis of the CT domain (*7*, *8*), but before doing so, the following two steps were taken. There were two *Bam*HI and *Eco*RV sites each in the overexpression plasmid. Each one was inside the ORF and the other, outside. Because these two inner restriction sites were to be used for subsequent gene manipulation, the outer sites needed to be removed. To remove the *Bam*HI site residing downstream of the ORF, the plasmid was digested with *Xho*I and *Xba*I flanking the *Bam*HI site. The resulting linear DNA was end-filled by nuclease treatment and self-ligated to give a truncated plasmid. To remove the *Eco*RV site located upstream of the ORF, the plasmid was digested with *Apa*I residing further upstream and treated successively with exonuclease and S1 nuclease. The resulting linear DNA was self-ligated to give a further truncated plasmid. Overexpression of PC was hardly affected by these truncations.

Asp543 and Glu576 were contained in the *Eco*RV and *Bam*HI fragment of 850 bp and Asp649, Lys712, Asp713, and Asp762 were in the *Bam*HI and *Bsp*1407I fragment of 710 bp (Figure 1). The codon for Glu592 overlaps the *Bam*HI site partially, and E592Q mutant was prepared in a way different from other mutants by one-step PCR. To ensure the replacement of these fragments with those with a mutation, they were replaced temporarily with a fragment of a different size, 1300 and 1200 bp for the former and the latter, respectively. The resulting working plasmids were termed PC-1300 and PC-1200, respectively.

Mutagenesis. Site-directed mutagenesis for all of the mutants but E592Q was carried out by two-step PCR with primers having a mutation at a desired position (Table 1). Thus, in the case of D543E, the first PCR was run with a combination of P-*Eco*RV and P-D543E-2 and of P-D543E-1 and P-*Bam*HI-1. The fragments thus amplified were recovered and allowed to anneal and extend. After the primers P-*Eco*RV and P-*Bam*HI-1 were added, the second PCR was run. The PCR conditions were as follows: After denaturation at 95 °C for 5 min, the samples were subjected to 30 cycles of denaturation (95 °C, 1 min), annealing (60 °C, 1.5 min), and extension (72 °C, 1.5 min) and subsequently subjected to an additional extension (72 °C, 10 min). After addition of the relevant primers, the samples were heated at 95 °C for 10 min, 30 °C for 15 min, and 72 °C for 3 min, followed by 30 cycles of denaturation (95 °C, 1 min), annealing (60 °C, 1 min), and extension (72 °C, 1 min). The pTrc99A-based overexpression plasmid was used as a template for PCR. PCR products were cloned into the TOPO vector for sequencing, and after confirmation of the proper mutation, the relevant fragment was replaced for the corresponding portion of PC-1300 or PC-1200 to give mutants of PC. The gene manipulations described above were carried out by standard methods (*9*).

Overexpression and Purification of Proteins. Escherichia coli JM109 transformed with either one of the overexpression plasmids prepared above was grown in LB medium supplemented with 50 μg/mL ampicillin and 1 μg/mL D-biotin. A fresh overnight culture (10 mL) from a single colony was used to inoculate 1 L of medium. The cultures were grown at 37 °C for 8−10 h, and then IPTG was added to a final concentration of 1 mM. The cultures were incubated for an additional 8−10 h. The cells were harvested by centrifugation at 5000 rpm (4200*g*) for 10 min at 4 °C. Proteins were purified according to the conventional procedures. In brief, the harvested cells were disrupted by sonication and centrifuged. The proteins were purified by ammonium sulfate fractionation and (diethylamino)ethyl (DEAE)-cellulose chromatography. Finally, PC was purified by monomeric avidin Sepharose affinity chromatography (*10*). The enzyme concentration was determined spectroscopically on the basis of the molar extinction coefficient 94 000 M^{-1} cm^{-1} at 280 nm for this PC (calculated molecular weight 128 528), as deduced from the content of aromatic amino acids (49 phenylalanines, 46 tyrosines, and 7 tryptophans).

Pyruvate Carboxylase Assays. Pyruvate carboxylase activity was measured by monitoring the oxalacetate formation using the coupled reaction with malate dehydrogenase according to the methods previously described (*8*, *11*). The oxidation of NADH in the malate dehydrogenase reaction was followed spectrophotometrically at 340 nm. All assays were carried out at 30 °C, and the reaction mixture contained the following components: 100 mM Tris-HCl (pH 8.0), 2 mM ATP, 100 mM $NaHCO_3$, variable concentration of pyruvate, 0.1 mM acetyl-CoA, 5 mM $MgCl_2$, 100 mM KCl, 0.15 mM NADH, 5 units of malate dehydrogenase, and 4−100 μg of PC in 1 mL. The kinetic parameters for pyruvate were determined by varying the pyruvate concentration from 0 to 50 mM at fixed concentrations of ATP and bicarbonate and by fitting the simple Michaelis−Menten equation to the data using EnzFitter (Biosoft, Cambridge, U.K.).

Oxamate-Induced Oxalacetate Decarboxylase Assays. Oxalacetate decarboxylase activity of wild-type PC and some of the mutants was measured with oxamate as the stimulant according to the procedures previously reported (*12*). The reactions were monitored by measuring the formation of pyruvate, which was then reduced to lactate by lactate dehydrogenase, and the concomitant oxidation of NADH was monitored at 340 nm. All assays were performed at 30 °C, and the reaction mixture contained the following components, unless otherwise stated: 100 mM Tris-HCl (pH 8.0), 5 mM $MgCl_2$, 100 mM KCl, 0.1 mM oxalacetate, 0.1 mM acetyl-CoA, 1 mM oxamate, 0.15 mM NADH, 5 units of lactate dehydrogenase, and 200−300 μg of PC in 1 mL. The reaction was started by the addition of wild-type or mutant PC, but prior to it, a background rate of oxalacetate decarboxylation was established, and this (2.4% of the maximum) was subtracted from the rate in the presence of an enzyme.

Table 1: Primers Used for Site-Directed Mutagenesis of the CT Domain of Pyruvate Carboxylase

name of primer	DNA sequence[a]
P-*Eco*RV	5′-GGA ATT *GAT ATC* GTC CAG TCG CAA ATT-3′
P-*Bam*HI-1	5′-TCC CAC *GGA TCC* TCT TTT AAA AAG CG-3′
P-*Bam*HI-2	5′-AGA *GGA TCC* GTG GGA TCG GCT TCT-3′
P-*Bsp*1407 I	5′-GCA *TGT ACA* CTT CCG TAT GCG G-3′
P-D543E-1	5′-GAC TGA TGA GC**C** **TC**C CGG AA-3′
P-D543E-2	5′-ACG ACG TTC CG**G** **GAG** GCT CAT CA-3′
P-E576D-1	5′-CAC AT**A** **TC**A AGC GA**G** AAT AAA TTC GGC-3′
P-E576D-2	5′-CGC TT**G** **AT**A TGT GGG GCG G-3′
P-E576Q-1	5′-CAC AT**T** **TG**A AGC GAG AAT AAA TTC GGC-3′ TTC
P-E576Q-2	5′-CGC TT**C** **AA**A TGT GGG GCG G-3′
P-E592Q	5′-ATC CC**A** C*GG ATC* ***C*****TG** TTT TAA AAA GCG-3′
P-D649N-1	5′-TTC CTT TCA CCC AG**T** TTA AAC T**GT** **T**GA AAA-3′
P-D649N-2	5′-CCA TGT GTT CCG AAT TTT C**AA** **C**AG TTT A-3′
P-K712R-1	5′-TAT C**TC** **T**AA TGG CCA AAA T**G**T GCG CAC-3′
P-K712R-2	5′-GGC CA**T** T**AG** **A**GA TAT GGC GGG-3′
P-K712Q-1	5′-TAT C**TT** **G**AA TGG CCA AAA TGT GCG CAC-3′
P-K712Q-2	5′-GGC CAT T**C** **A**GA TAT GGC GGG-3′
P-D713E-1	5′-GCC CCG C**C**A T**TT** **C**TT TAA TGG CCA AAA T-3′
P-D713E-2	5′-GGC CAT TAA A**G** **A**AT GGC GGG G-3′
P-D713N-1	5′-GCC CCG CCA T**AT** **T**TT TAA TGG CCA AAA T-3′
P-D713N-2	5′-GGC CAT TAA A**AA** **T**AT GGC GGG G-3′
P-D762E-1	5′-ACA AT**T** **TC**A A**C**G CCG GCT TCA ATC GCT-3′
P-D762E-2	5′-GAA GC**C** GGC GTT **GAA** ATT GTT GAT GTC-3′
P-D762N-1	5′-ACA ATA **TT**A ACG CC**G** GCT TCA ATC GCT-3′
P-D762N-2	5′-GAA GCC G**G**C GTT **A**AT ATT GTT GAT GTC-3′

[a] The codon shown in bold represents the amino acid subjected to mutagenesis, and the underlined base represents the one mutated. Restriction enzyme sites are shown in italics.

Kinetic parameters for oxalacetate were determined by varying its concentration from 0 to 1 mM at a fixed oxamate concentration of 1 mM. In this reaction, inhibition by the substrate was manifest, and hence the data were analyzed by eq 3, which takes substrate inhibition into account, where K_I represents the substrate inhibition constant. On the other hand, kinetic parameters for oxamate were determined by varying its concentration from 0 to 5 mM at a fixed oxalacetate concentration of 0.1 mM. A weak oxalacetate decarboxylase activity was observed even in the absence of oxamate (10% of the maximum), and the decarboxylase activity, too, was subject to substrate inhibition. Accordingly, the data were analyzed by eq 4, which takes substrate inhibition into account, where v_0 represents the rate in the absence of oxamate.

$$v = V_{max}[S]/([S] + K_m + [S]^2/K_I) \quad (3)$$

$$v = V_{max}[S]/([S] + K_m + [S]^2/K_I) + v_0 \quad (4)$$

Measurement of pH-Rate Profiles for Pyruvate Carboxylase and Oxalacetate Decarboxylase Reactions. To construct a pH-rate profile, enzymatic activity of wild-type PC and mutants D543E and D649N was determined at a different pH from 5 to 9 at a fixed substrate concentration. The buffer used was a mixture of 50 mM Bis-Tris, 25 mM Tricine, and 25 mM glycine, which is a constant ionic strength buffer system (*12*). The pyruvate carboxylase activity was determined at a specified pH under the standard conditions described above except for the use of 50 mM pyruvate for the D543E mutant. Likewise, the oxalacetate decarboxylase activity was determined at a specified pH under the standard conditions.

Assay for Tritium Release from Tritiated Pyruvate. Preparation of tritiated pyruvate and release of tritium from pyruvate were carried out in the same way as those described previously (*13*, *14*). Thus, the reaction solution (0.50 mL) for tritium release contained the following components: 100 mM Tris-HCl (pH 8.0), 10 mM [3-^{3}H]pyruvate (37 000 cpm/μmol), 2 mM ATP, 100 mM $NaHCO_3$, 0.1 mM acetyl-CoA, 5 mM $MgCl_2$, 100 mM KCl, and 2−250 μg of PC. The reaction was run for 15 min at 30 °C and terminated by the addition of trichloroacetic acid to 3% (w/v). The mixture was centrifuged at 14 000 rpm for 1 min, and the supernatant was neutralized with KOH. The solution was applied to a column (gel volume = 6 mL) of Dowex 1 (chloride form) and washed with deionized water. A total of 1 out of 10 mL of the effluent was mixed with 10 mL of scintillation cocktail, scintisol 500 (Dojindo, Kumamoto, Japan), and the radioactivity was determined with a Beckman Coulter LS 6500 scintillation counter. The readings in counts per minute were divided by the quantity of protein used (milligrams) for comparison of the relative rate of release among the enzymes. All experiments were carried out three times, and the values presented are the mean with standard deviations.

Determination of Association States by HPLC Gel-Filtration Chromatography. High-performance gel-filtration chromatography was run on a TSK gel G3000SWXL column (7.8 mm × 30 cm) with a TSK guard column SWXL (6.0 mm × 4.0 cm) (Tosoh, Tokyo, Japan) using an HPLC system (Hitachi, Tokyo, Japan). The samples were eluted at a flow rate of 0.5 mL/min with a 100 mM KPi buffer (pH 7.0) containing 100 mM Na_2SO_4 as the mobile phase, and the eluted samples were monitored at 280 nm. The gel-filtration column was calibrated using a set of standard proteins (Amersham): ribonuclease A (13.7 kDa), chymotrypsinogen A (23 kDa), ovalbumin (43 kDa), albumin (67 kDa), aldolase (158 kDa), and thyroglobulin (669 kDa). The apparent molecular weights of the samples were estimated from the calibration curve obtained. The samples were analyzed at

concentrations ranging from 5 to 100 μM, and 20 μL each was applied to the column.

Circular Dichroism (CD) Spectroscopy. Protein samples for CD measurements were dialyzed overnight against a 100 mM KPi buffer (pH 7.0) containing 100 mM Na_2SO_4. CD spectra of wild-type and mutant PC were determined in the above buffer at ambient temperature (20 °C) on a spectropolarimeter, model J-725, Jasco, Tokyo, Japan. The sample concentration was 5 μM, and a 1-mm path-length cuvette was used. CD spectra were obtained by collecting data points from 200 to 290 nm in 0.5-nm increments. Each spectrum was calibrated by subtracting the background spectrum with the buffer. Thermal denaturation curves were obtained by monitoring the ellipticity at 222 nm in the temperature range from 20 to 80 °C. The denaturation temperatures of proteins were estimated by differentiating the thermal denaturation curves.

RESULTS

Selection of the Targets for Mutagenesis of the CT Domain. It is relatively easy to define the CT domain of PC, especially for the N terminus, because subunit-type PC is present with its BC domain constituting a separate subunit (*6*). Thus, the sequence from amino acid numbers 509−1050 was regarded to constitute the CT domain of *B. thermodenitrificans* PC. It was found that the following amino acids with numbers in parentheses are conserved over this region among 41 species whose sequences were available as of March, 2003: Asp (4), Glu (2), Lys (1), His (2), Gln (1), Ser (2), Thr (1), Arg (4), Gly (5), Ala (1), Leu (2), Pro (2), Phe (1), and Trp (1). Of them, the nonpolar amino acids, Gly, Ala, Leu, Pro, and Phe, may be excluded from a candidate of catalytic residues. The polar amino acids were divided according to the acidity of the side-chain group; Asp, Glu, Lys, and His possess those with moderate acidity (pK_a 3−10), whereas the side-chain groups of the rest of the amino acids show weaker acidity. The amino acids in the former group were given a priority as a candidate of catalytic residues. If we assume further that, despite poor sequence homology, all of the biotin-dependent carboxylases mediate carboxyl transfer by an identical or similar mechanism, catalytic residues may be common to all of them. If this assumption holds, His can be excluded, because there is no conserved His in ACC, leaving the following residues as targets for mutagenesis of the CT domain of PC: Asp543, Glu576, Glu592, Asp649, Lys712, Asp713, and Asp762. Aspartates were converted either to asparagine or glutamate, glutamates to glutamine or aspartate, and lysine to arginine or glutamine. The mutants actually prepared are summarized in Table 2.

Purification of PC Mutants. All of the mutants of PC were overexpressed in *E. coli* to the same extent as the wild-type enzyme and purified in a way identical to that for wild-type PC. Most of them were expressed in soluble form, but D543N and D649E mutants were kept in the inclusion body and resisted purification. The enzymatic activity was not detectable for them, but it is not known whether it was their intrinsic property or because of the improper handling of the proteins. Each of the purified proteins was nearly homogeneous as judged by visual inspection of SDS−PAGE; in each case, the protein band was observed at the position (128 kDa) expected from their molecular size deduced from the DNA sequences. Each of the soluble proteins was obtained in a yield of 8 mg from a 2-L culture on average.

Table 2: Kinetic and Physicochemical Properties of Wild-Type and Mutated PCs

protein	kinetic parameters for pyruvate carboxylase reaction[a] V_{max} (U/mg)[b]	K_m (mM) for pyruvate	association state[c]	denaturation temperature (°C)
wild type	9.88 ± 0.29	0.30 ± 0.03	T	70.0
D543E	0.46 ± 0.03	16.2 ± 2.4	T	69.5
E576D	2.47 ± 0.12	0.44 ± 0.08	T	70.0
E576Q	0.30 ± 0.02	1.62 ± 0.24	T, D, M	68.0
E592Q	1.67 ± 0.15	0.49 ± 0.15	T, D, M	
D649N	0.19 ± 0.02	1.20 ± 0.27	T	70.0
K712R	0.096 ± 0.004	0.41 ± 0.07	T	70.0
K712Q	*d*	*d*	T	70.5
D713E	2.03 ± 0.06	0.58 ± 0.05	T, D, M	
D713N	1.46 ± 0.12	1.16 ± 0.26	T, D, M	
D762E	9.13 ± 0.24	0.29 ± 0.03	T	
D762N	4.14 ± 0.10	0.28 ± 0.02	T	

[a] The kinetic parameters and their standard errors were determined by nonlinear regression analysis of the saturation curves as described in the Experimental Procedures. [b] One unit of enzyme activity was defined as the amount of enzyme required to catalyze the formation of 1 μmol of oxalacetate per min. [c] T, D, and M stand for tetramer, dimer, and monomer, respectively. [d] Accurate kinetic parameters could not be determined, because the activity was smaller than 0.001 U/mg even under substrate saturation conditions.

Pyruvate Carboxylase Activity of CT Mutants. Kinetic parameters for the carboxylation of pyruvate by wild-type PC and its mutants are summarized in Table 2. The V_{max} values of all of the mutants were generally smaller than that of the wild type, but they could be grouped into three according to their magnitude of decrease. The first group comprised D543E, E576Q, D649N, K712R, and K712Q, which lost over 95% of the activity of the wild-type enzyme. Especially, virtually no activity was found for K712Q, and the activity of K712R was lowered greatly, indicating that even the homologous substitution of Lys712 is not tolerated for the enzyme to be active. It is also noted that the K_m of D543E for pyruvate increased 50 times, suggesting that it is located in the binding site for this substrate. The second group comprised E576D, E592Q, D713E, and D713N, whose extent of the loss of enzymatic activity remained medium (10−25%). The third group comprised D762E and D762N, whose loss of activity was insignificant (<40%). Rather unexpectedly, the K_m for pyruvate of all but D543E changed less than 6 times. These kinetic data suggest that Lys712, Asp543, Glu576, and Asp649 are of particular importance in the carboxyl transfer of PC to pyruvate.

Determination of the Association States by HPLC Gel-Filtration Chromatography. Association states of wild-type PC and its mutants were investigated by high-performance gel-filtration chromatography. Apparent molecular weights of the samples were estimated on the basis of the calibration curve constructed with a set of standard proteins. Typical elution profiles for wild-type PC and some of the mutants are shown in Figure 2, and the association states estimated from the retention times are compiled in Table 2. As expected, wild-type PC was found to exist mainly as a tetramer, which is typical for single polypeptide-type PCs (*2*, *3*). With mutants E592Q, D713E, and D713N with the activity decrease of medium magnitude, the enzyme tends

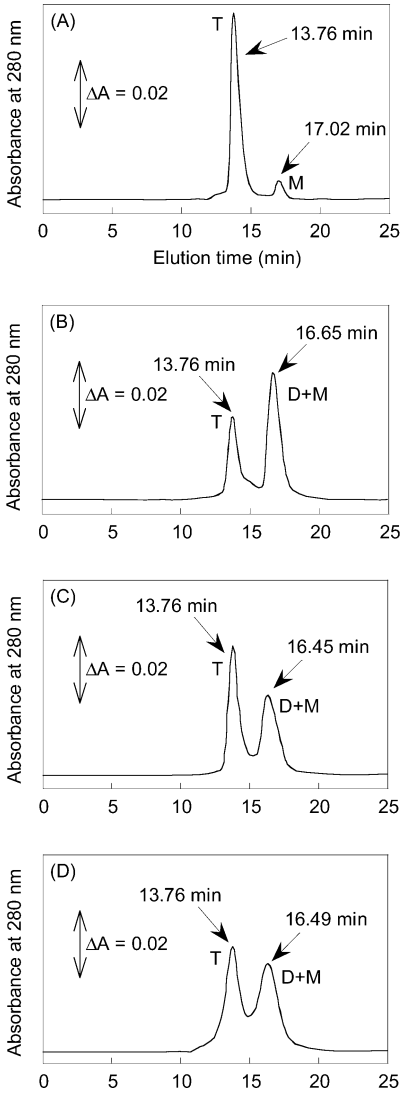

FIGURE 2: Typical elution profiles for wild-type PC (A), E576Q (B), E592Q (C), and D713E (D) on the TSK G3000SWXL gel-filtration column. The concentration of the samples injected varied from 5 to 100 μM, and the sample shown here is for 20 μM. M, D, and T denote monomer, dimer, and tetramer, respectively.

to dissociate to either dimers or monomers. The proportion of the tetramer varied from 60 (E592Q) to 40% (D713E), but because it was reported that the tetrameric form is essential for PC to be fully active (*15*), this dissociation seems to be responsible at least in part for the decrease in activity. In contrast to these mutants, D543E, D649N, K712R, and K712Q, which lost most of the activity in the overall reaction, were present in the tetrameric form just like wild-type PC (data not shown). An exception was mutant E576Q, which underwent dissociation to dimers or monomers to the greatest extent of the mutants tested (Figure 2), and the decrease in activity of this mutant seems to be due to a structural deformation.

CD Studies. To further probe the probable structural changes in the PC mutants, CD spectra were determined. Wild-type PC gave a rise in absorption at 222 nm with a molar ellipticity of -1.2×10^4 deg cm dmol^{-1}. The CD spectra of D543E and K712Q were superimposable to that of wild-type PC, demonstrating that any large structural change had not occurred to them. In E576Q, which underwent dissociation markedly, the molar ellipticity at 222 nm was the same, but that at 210 nm was 6% smaller than that of the wild type.

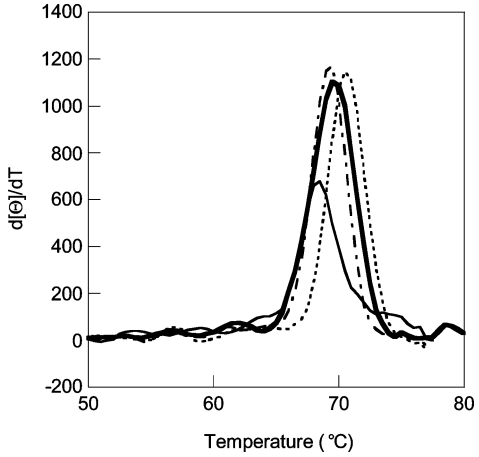

FIGURE 3: First-order derivative of the thermal denaturation curves of wild-type PC (—) and its CT mutants, E576Q (−), D543E (− · −), and K712Q (·····).

Thermal stability of some of the mutants was estimated from a decrease in molar ellipticity at 222 nm with temperature. The raw data were transformed by taking the first-order derivative of the denaturation curve (Figure 3). The denaturation temperature thus obtained, 70 ± 0.5 °C, was hardly different among the wild-type PC and D543, D649, and K712 mutants (Table 2), demonstrating that the thermal stability was minimally affected by the mutation in these mutants. In contrast, the denaturation temperature of E576Q was lower by 2 °C, and the enthalpy of denaturation was one-half those of other proteins. This phenomenon may be interpreted as suggesting that the structure of E576Q protein is partially broken even before heating. This notion is consistent with the observation in HPLC that E576Q was prone to dissociation most markedly. When taken together, a structural change seems to be responsible for the decrease in the activity of E576Q, and Glu576 does not seem to participate in catalysis directly.

Oxamate-Induced Oxalacetate Decarboxylase Activity of the CT Mutants. Oxamate-induced decarboxylation of oxalacetate by wild-type PC and some of the mutants was also studied. It was found that the activity of the K712 mutants was lost nearly completely, just like that of the overall reaction (data not shown). Kinetic parameters of the wild-type PC and D543 and D649 mutants for oxalacetate and oxamate are summarized in Table 3. Just like in the carboxylation of pyruvate, a considerable decrease in V_{max} was observed for these mutants from that of the wild-type enzyme, but the magnitude of decrease was less marked. Presumably, the rate-limiting step of the oxamate-induced oxalacetate decarboxylation lies not in the carboxyl transfer to biotin from oxalacetate but in the subsequent decarboxylation of carboxybiotin induced by oxamate (*12*). In other words, the decarboxylation of carboxybiotin is the rate-determining step in wild-type PC, whereas the carboxyl transfer from oxalacetate to biotin may be the rate-determining step with the mutants as a result of a decrease in their catalytic activity for this process. This shift of the rate-determining step between the wild type and the mutants may be responsible for the difference in the extent of decrease in the activity between them. On the other hand, a marked

Table 3: Kinetic Parameters for Oxamate-induced Oxalacetate Decarboxylase Reaction[a]

	parameters for oxalacetate[b]			parameters for oxamate[c]		
protein	V_{max}[d] (mU/mg)	K_m (mM)	K_I (mM)	V_{max}[d] (mU/mg)	K_m (mM)	K_I (mM)
wild type	46.3 ± 5.8	0.019 ± 0.006	0.32 ± 0.09	44.1 ± 6.9	0.57 ± 0.16	5.4 ± 2.1
D543E	10.5 ± 1.4	0.033 ± 0.008	0.14 ± 0.03	8.25 ± 0.63	0.80 ± 0.10	4.6 ± 0.8
D649N	3.36 ± 0.30	0.027 ± 0.005	0.18 ± 0.03	2.80 ± 0.35	0.47 ± 0.11	3.1 ± 0.8

[a] The kinetic parameters and their standard errors were determined by nonlinear regression analysis of the saturation curves as described in the Experimental Procedures. [b] The concentration of oxalacetate was varied from 0 to 1 mM at a fixed oxamate concentration of 1 mM. [c] The concentration of oxamate was varied from 0 to 5 mM at a fixed oxalacetate concentration of 0.1 mM. [d] One unit of enzyme activity was defined as the amount of enzyme required to catalyze the formation of 1 μmol of pyruvate per min.

difference was not seen for the K_m and K_I for oxalacetate and oxamate. Nevertheless, the K_m of the D543E mutant for oxalacetate and oxamate increased slightly, demonstrating that the binding of oxalacetate and oxamate as well as pyruvate is impaired more or less by this mutation.

pH Dependence of the Enzymatic Activity. To gain more insight into the catalytic residues of PC, a pH-rate profile was taken for the carboxylation of pyruvate mediated by the wild-type enzyme. The profile is nearly identical to that for *B. thermodenitrificans* PC with a rate maximum around pH 8−8.5 (*16*), suggesting that a pair of amino acid residues and/or substrates with a pK_a around 7−9 is involved in the reaction. Care should be taken, however, when interpreting these data, because the overall reaction of PC is composed of two partial reactions, eqs 1 and 2, and the profile must represent their sum. To extract the CT reaction from it, a pH-rate profile for the decarboxylation of oxalacetate was also studied. In sharp contrast to the forward reaction, the activity was independent of pH. A similar phenomenon was observed for the chicken enzyme (*12*), suggesting that the pH-rate profile observed represents that of the former partial reaction. The pH independence of the CT reaction may be interpreted by one of the following two explanations. The catalytic residue(s) involved in the carboxyl transfer may not possess a pK_a in the pH range of 5−9 that was studied. This explanation is compatible with our notion that the aspartate, glutamate, and lysine residues are involved in the carboxyl transfer. Alternatively, amino acid residues bearing an ionic group may not be involved in the reaction, but the carboxyl group is transferred directly from biotin to pyruvate. As far as our mutagenetic data that suggest the mutation of aspartate and lysine impairs the catalytic activity markedly are concerned, the former explanation seems more plausible.

pH-rate profiles of similar shape were obtained for mutants D543E and D649N, though the absolute values were much smaller. These observations may be understandable, because the pK_a of the residues in question, aspartate and lysine, is outside of the pH range of 5−9. To gain more information on the catalytic aspartate(s), experiments at pH lower than 5 were attempted, but reliable data were not obtained presumably because of the instability of the enzyme.

Tritium Release from Tritiated Pyruvate. It was reported that the release of tritium from tritiated pyruvate occurs only in the presence of the complete reaction mixture (*13*). These kind of experiments may provide a clue toward discriminating the exact role of Asp543 and Asp649, and hence the tritium-release assay was carried out with D543E and D649E as well as wild-type PC. The rates of carboxylation of pyruvate were 9.72 ± 0.32, 0.16 ± 0.016, and 0.18 ± 0.015 U/mg for wild type, D543E, and D649E, respectively (mean ± standard deviation from the three determinations), with 10 mM pyruvate at 30 °C and pH 8.0. The rates of tritium release from tritiated pyruvate were 47 700 ± 4700, 1060 ± 190, and 1330 ± 210 cpm/mg, with the respective enzymes under identical conditions. In other words, upon mutation of Asp543 and Asp649, the rate of tritium release was diminished drastically just like that of the carboxylation of pyruvate, while the extent of decrease was nearly the same in both mutants, D543E and D649N. The implications of these observations are discussed below.

DISCUSSION

Although much less is known about the mechanism of carboxyl transfer involving biotin in the reaction of PC than that of the carboxylation of biotin, several models have been proposed for it (*17*). At first, carboxylation of pyruvate was supposed to proceed in a concerted manner based on an observation that the configuration of the methyl group was retained upon carboxylation (*18*). More recently, however, it was claimed that a stepwise mechanism is more plausible based on the kinetic isotope effects on the decarboxylation of oxalacetate, in which the proton and carboxyl transfers take place in discrete steps and an acid/base pair participates in these processes (*19*). The first step would be the abstraction of a proton from the methyl group of pyruvate by the base. Subsequently, the acid assists the carboxyl transfer by facilitating polarization of the ureido group of biotin. On the basis of the chemical modification experiments on PC, a lysine−cysteine pair was postulated as a candidate for this (*19*, *20*).

Consistent with this hypothesis, there is indeed a conserved lysine residue in the CT domain of PC, and its substitution with arginine or glutamine nearly abolished the catalytic activity of PC (Table 2). In contrast, there is no conserved cysteine in the CT domain, and the possibility that cysteine participates in the carboxyl transfer seems vanishingly small. The cysteine hypothesis was based on an observation that the treatment of PC with *o*-phthalaldehyde resulted in a large reduction in the oxamate-induced decarboxylation of oxalacetate (*20*). The interpretation of these data is not straightforward, however, as the authors themselves admitted, and other possibilities such as steric hindrance rather than the modification of catalytic residues need to be taken into account. Our results of the site-directed mutagenesis revealed that Asp543 and Asp649 are indispensable in the overall reaction of PC (Table 2), and either of them may be playing the role that cysteine was supposed to do. Hence, It is proposed that the original lysine−cysteine hypothesis be changed to a lysine−aspartate theory.

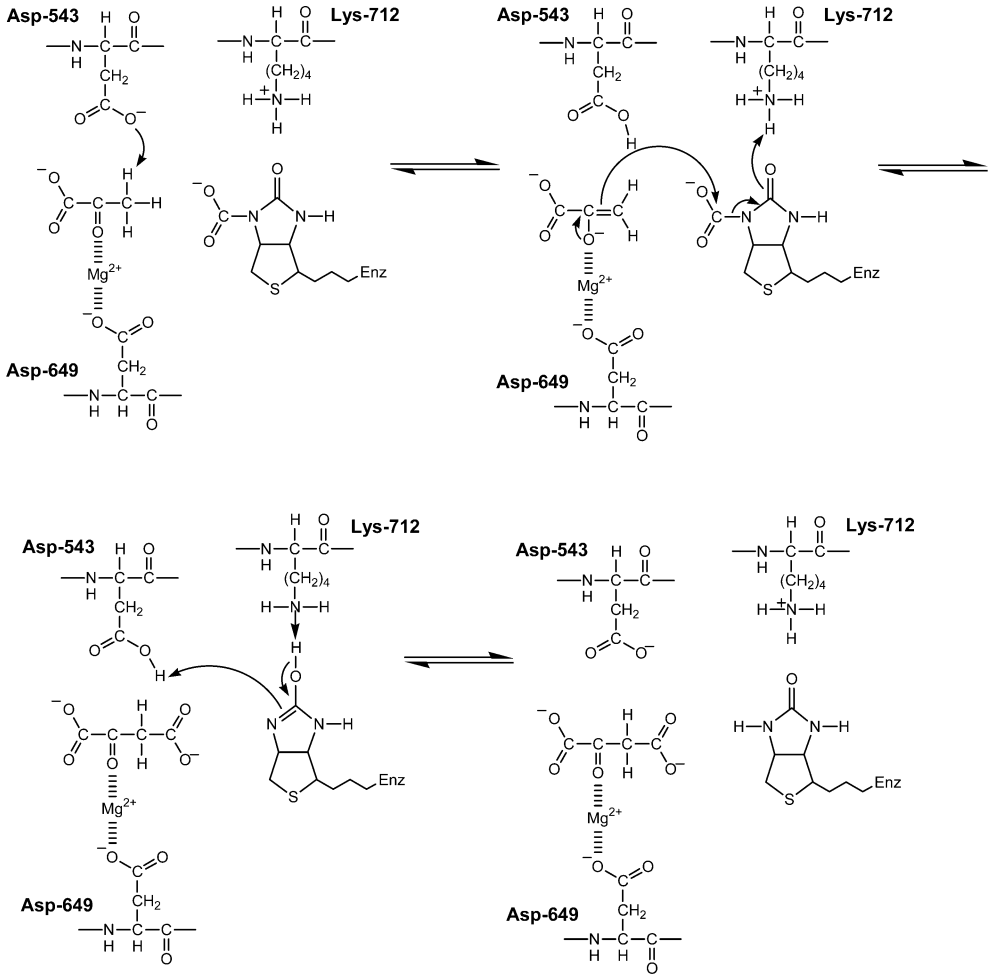

FIGURE 4: Proposed model for the carboxyl transfer in the PC reaction, in which Lys712 and Asp543 serve as key catalytic residues.

The specific functions of Lys712, Asp543, and Asp649 are discussed as follows: On the basis of the acidity of the amino group of lysine and the carboxyl of aspartate, it would be reasonable to assume that the former exists in the protonated form and the latter, in the deprotonated form under physiological conditions. It is conceivable that one of the aspartate residues is engaged in the abstraction of a proton from the methyl group of pyruvate. This step may be rate-determining of the whole process, and hence, once this residue is converted to catalytically incompetent asparagine, the enzymatic activity will be abolished. In fact, the activity of D649N decreased sharply to 2% of that of the wild type but was not completely lost, suggesting that Asp649 may not be the base abstracting a proton. Rather, Asp543 may play this role, because a significant decrease in the activity was observed upon mutation of this residue into homologous glutamate (D543E, 5% of wild type). This notion may be consistent with the observation that the K_m of D543E for pyruvate increased 50-fold, suggesting that Asp543 is located in the pyruvate-binding site. As for the function of Asp649, the following role may be assigned. It was suggested that there is a divalent metal ion, most probably Mn^{2+}, at the active site of CT (*4*). Because an excess of magnesium ion is present in our assay system, it may play a role that manganese is supposed to do, i.e., stabilization of the incipient enolate ion by coordinating to the carbonyl oxygen of pyruvate to form a ternary complex involving Asp649. In other words, Asp649 helps anchor the metal in correct orientation at the active site, thereby indirectly assisting the reaction to proceed smoothly. The observation that the rate of tritium release from pyruvate is not different significantly between mutants D543E and D649E is not contradictory to these arguments because Asp649 participates, albeit indirectly, in the proton abstraction from pyruvate. Its mutation would exert the same adverse effect as does the mutation of Asp543.

On the basis of these arguments, a mechanism depicted in Figure 4 is proposed for the carboxyl transfer of PC, where Lys712 and Asp543 serve as the key acid and base catalyst, respectively. The reaction begins with the abstraction of a proton from the methyl group of pyruvate by Asp543 to form an enolate or enol. This process is facilitated by Mg^{2+} coordinated to Asp649. The resulting enolate undergoes nucleophilic attack on the carboxylbiotin, and this process is facilitated by a proton donation to the ureido oxygen of biotin by Lys712. In this scheme, the attack is supposed to occur directly on the carboxylbiotin, but an alternative mechanism where the attack occurs on carbon dioxide released from it is not ruled out. The enol (isourea) form of biotin thus generated transiently returns to the more thermodynamically stable keto (ureido) form by abstracting a proton from Asp543. The electrostatic repulsion between the carboxylates of Asp543 and oxalacetate may be the driving force to repel the product from the active site.

As described above, Asp543 seems to participate in the binding of pyruvate. In the 5S subunit of transcarboxylase,

whose reaction is identical to that of CT of PC, a region comprising Trp73 was postulated as the site of pyruvate binding (*6*). Trp595 corresponds to this residue in *B. thermodenitrificans* PC, and Glu592 is present in its vicinity. If Trp595 is indeed involved in pyruvate binding, Glu592 may be more or less. This possibility seems remote, however, as far as our mutagenetic data are concerned, because a mutation of Glu592 exerted only a minor effect on the activity and pyruvate binding (Table 2). Instead, Asp543 located far away from Trp595 in terms of the primary structure might come close to the latter three-dimensionally to constitute the pyruvate-binding site. The validity of this hypothesis awaits elucidation of the three-dimensional structure of PC, which is under way in this laboratory.

It was reported previously that there is a region in the CT domain of PC that shows sequence homology equal to that of pyridoxal phosphate-dependent serine/threonine dehydratase (*6*). Lys712 is present in it, and its dehydratase counterpart plays multiple roles in the catalysis; this key lysine not only attaches to the cofactor covalently, but also can presumably serve as a base to abstract a proton from the substrate (*21*). The product of dehydration of serine is pyruvate, which is the substrate in the reaction of PC. Nothing more can be said with certainty at the present time, but this portion of the two proteins might have evolved from a common ancestor.

Although it seems certain that key catalytic residues have been identified in this paper, it is not intended to assert that other residues do not participate in the carboxyl transfer reaction. In many enzymatic reactions, histidine constitutes part of the catalytic machinery, arginine is often involved in the binding of anionic substrates, and they can be equally as important as those identified above. The function of these and several other amino acids such as serine and threonine needs to be assessed experimentally.

Finally, the relevance of the mechanism of PC to those of other related enzymes is discussed briefly. Recently, the three-dimensional structure of the CT domain of yeast ACC was reported (*22*). Although the mode of reaction is essentially the same for the CTs of ACC and PC, their amino acid sequences are barely homologous, and hence, it is hard to know whether the catalytic mechanism and key residues are identical or not in the two enzymes. There are indeed two conserved lysine and four aspartate residues, as well as several arginines, near the CoA-binding site in the putative active site cavity of CT of yeast ACC, and it seems possible that some of them play a role similar to that in PC. Another enzyme whose reaction resembles that of CT of PC is phosphoenolpyruvate (PEP) carboxylase. According to the three-dimensional structure of *E. coli* PEP carboxylase (*23*) and mutagenetic studies (*24*), two histidine residues seem to participate in catalysis, but there are also one conserved lysine and five aspartate residues near the histidines. Two possibilities may be easily raised for their function: one or more of them constitutes a part of the catalytic machinery of this enzyme, or alternatively, none of them is involved directly in catalysis, despite apparent similarities in the mode of the reaction. If the latter hypothesis turns out to be the case, key catalytic residues and the overall reaction mechanism are to be different between the two systems, biotin-dependent carboxylases and PEP carboxylase, despite apparent similarities in the mode of the reaction. In the reaction of PEP carboxylase, the acceptor substrate is already in the reactive enol form, and a base required to abstract a proton from the methyl group of pyruvate in the reaction of CT of PC will not be needed in PEP carboxylase. In addition, the donor substrate is bicarbonate rather than carboxylbiotin in PEP carboxylase. These subtle differences could be the result of such a difference in the mechanisms of the two enzymes.

REFERENCES

1. Utter, M. F., and Keech, D. B. (1960) Formation of oxalacetate from pyruvate and carbon dioxide, *J. Biol. Chem. 235*, 17−18.
2. Jitrapakdee, S., and Wallace, J. C. (1999) Structure, function, and regulation of pyruvate carboxylase, *Biochem. J. 340*, 1−16.
3. Barden, R. E., Taylor, B. L., Isohashi, F., Frey, W. H., II, Zander, G., Lee, J. C., and Utter, M. F. (1975) Structural properties of pyruvate carboxylases from chicken liver and other sources, *Proc. Natl. Acad. Sci. U.S.A. 72*, 4308−4312.
4. Wood, H. G., and Barden, R. E. (1977) Biotin enzymes, *Annu. Rev. Biochem. 46*, 385−413.
5. Lim, F., Morris, C. P., Occhiodoro, F., and Wallace, J. C. (1988) Sequence and domain structure of yeast pyruvate carboxylase, *J. Biol. Chem. 263*, 11493−11497.
6. Mukhopadhyay, B., Stoddard, S. F., and Wolfe, R. S. (1998) Purification, regulation, and molecular and biochemical characterization of pyruvate carboxylase from *Methanobacterium thermoautotrophicum* strain Δ*H*, *J. Biol. Chem. 273*, 5155−5166.
7. Kondo, H., Kazuta, Y., Saito, A., and Fuji, K. (1997) Cloning and nucleotide sequence of *Bacillus stearothermophilus* pyruvate carboxylase, *Gene 191*, 47−50.
8. Sueda, S., Islam, M. N., and Kondo, H. (2004) Protein engineering of pyruvate carboxylase. Investigation on the function of acetyl-CoA and the quaternary structure, *Eur. J. Biochem. 271*, 1391−1400.
9. Sambrook, J., Fritsch, E. F., and Maniatis, T. (1989) *Molecular Cloning: A Laboratory Manual*, 2nd ed., Cold Spring Harbor Laboratory, Cold Spring Harbor, NY.
10. Jitrapakdee, S., Walker, M. E., and Wallace, J. C. (1999) Functional expression, purification, and characterization of recombinant human pyruvate carboxylase, *Biochem. Biophys. Res. Commun. 266*, 512−517.
11. Modak, H. V., and Kelly, D. J. (1995) Acetyl-CoA-dependent pyruvate carboxylase from the photosynthetic bacterium *Rhodobacter capsulatus*: rapid and efficient purification using dye-ligand affinity chromatography, *Microbiology 141*, 2619−2628.
12. Attwood, P. V., and Cleland, W. W. (1986) Decarboxylation of oxalacetate by pyruvate carboxylase, *Biochemistry 25*, 8181−8196.
13. Mildvan, A. S., Scrutton, M. C., and Utter, M. F. (1966) Pyruvate carboxylase. VII. A possible role for tightly bound manganese, *J. Biol. Chem. 241*, 3488−3498.
14. Rose, Z. B. (1960) Studies on the mechanism of action of isocitric dehydrogenase, *J. Biol. Chem. 235*, 928−933.
15. Khew-Goodall, Y. S., Johannssen, W., Attwood, P. V., Wallace, J. C., and Keech, D. B. (1991) Studies on dilution inactivation of sheep liver pyruvate carboxylase, *Arch. Biochem. Biophys. 284*, 98−105.
16. Cazzulo, J. J., Sundaram, T. K., and Kornberg, H. L. (1970) Properties and regulation of pyruvate carboxylase from *Bacillus stearothermophilus*, *Proc. R. Soc. London, Ser. B 176*, 1−19.
17. Knowles, J. (1989) The mechanism of biotin-dependent enzymes, *Annu. Rev. Biochem. 58*, 195−221.
18. Retey, J., and Lynen, F. (1965) On the biochemical function of biotin. IX. The steric course in the carboxylation of propionyl-CoA, *Biochem. Z. 342*, 256−271.
19. Attwood, P. V., Tipton, P. A., and Cleland, W. W. (1986) Carbon-13 and deuterium isotope effects on oxalacetate decarboxylation by pyruvate carboxylase, *Biochemistry 25*, 8197−8205.
20. Werneburg, B. G., and Ash, D. E. (1993) Chemical modifications of chicken liver pyruvate carboxylase: evidence for essential cysteine-lysine pairs and a reactive sulfhydryl group, *Arch. Biochem. Biophys. 303*, 214−221.

21. Gallagher, D. T., Gilliland, G. L., Xiao, G., Zandlo, J., Fisher, K. E., Chinchilla, D., and Eisenstein, E. (1998) Structure and control of pyridoxal phosphate dependent allosteric threonine deaminase, *Structure 6*, 465−475.
22. Zhang, H., Yang, Z., Shen, Y., and Tong, L. (2003) Crystal structure of the carboxyltransferase domain of acetyl-coenzyme A carboxylase, *Science 299*, 2064−2067.
23. Kai, Y., Matsumura, H., Inoue, T., Terada, K., Nagara, Y., Yoshinaga, T., Kihara, A., Tsumura, K., and Izui, K. (1999) Three-dimensional structure of phosphoenolpyruvate carboxylase: a proposed mechanism for allosteric inhibition, *Proc. Natl. Acad. Sci. U.S.A. 96*, 823−828.
24. Terada, K., Murata, T., and Izui, K. (1991) Site-directed mutagenesis of phosphoenolpyruvate carboxylase from *E. coli*: the role of His579 in the catalytic and regulatory functions, *J. Biochem. 109*, 49−54.

BI035783Q